Bioorganic & Medicinal Chemistry 20 (2012) 769–774

Contents lists available at SciVerse ScienceDirect

Bioorganic & Medicinal Chemistry

journal homepage: www.elsevier.com/locate/bmc

Switchable MRI contrast agents based on morphological changes of pH-responsive polymers

Satoshi Okada [a], Shin Mizukami [a,b], Kazuya Kikuchi [a,b,*]

[a] Division of Advanced Science and Biotechnology, Graduate School of Engineering, Osaka University, 2-1 Yamadaoka, Suita, Osaka 565-0871, Japan
[b] Immunology Frontier Research Center, Osaka University, 3-1 Yamadaoka, Suita, Osaka 565-0871, Japan

ARTICLE INFO

Article history:
Received 26 October 2011
Revised 30 November 2011
Accepted 1 December 2011
Available online 8 December 2011

Keywords:
MRI
Contrast agent
pH-responsive polymer
Rotational correlation time
Molecular switch

ABSTRACT

Magnetic resonance imaging (MRI) contrast agents are effective tools in both medical diagnosis and life science research. Various smart contrast agents have been developed for the visualization of biological phenomena. These contrast agents have molecular switches that increase or reduce MRI signal intensity in response to the target biological reaction. Therefore, novel approaches to the design of molecular switches for versatile in vivo studies using MRI are eagerly anticipated. Here, we report one such approach for the development of molecular switches based on morphological changes of pH-responsive polymers. We designed and synthesized three types of contrast agents based on a linear homopolymer or spherical copolymers with two different cross-linking degrees. The relaxivity measurements showed that these agents have molecular switches that respond to pH changes, and fluorescence studies indicated that these switches are based on the alteration of the molecular tumbling caused by pH-responsive morphological changes. As a result, the spherical polymers possess promising characteristics for the development of switchable MRI contrast agents.

1. Introduction

Magnetic resonance imaging (MRI) is a useful imaging method because it allows for the noninvasive visualization of living tissues with high spatial and temporal resolution. MRI contrast agents (CAs) are widely used in medical diagnosis to improve the tissue contrast by shortening the longitudinal relaxation time (T_1) and the transverse relaxation time (T_2) of water protons. T_1 and T_2 shortening efficiencies of the CA are described as T_1 relaxivity (r_1) and T_2 relaxivity (r_2), respectively.[1,2] Thus, higher relaxivity means higher sensitivity of the CA, which results in significant changes in the MRI signal intensity.

Recently, switchable CAs have been used to detect enzyme reactions,[3,4] metal ions,[5,6] and pH alteration.[7–10] These so-called 'smart' CAs contain molecular switches, which cause their relaxivities to change in response to the targeted biological reaction. One common approach to the development of molecular switches is to change the coordination number of water molecules. In this case, the coordination of a water molecule with the paramagnetic ion is obstructed by the removable or coordinating group.[3,5,6] After stimulation, these hindrances to the coordination of the water molecule are eliminated, and the relaxivity increases. Another approach is based on the molecular tumbling of the CA. It is known that the rotational correlation time (τ_R), which is an indicator of the velocity of molecular tumbling in the solution, affects the relaxivity. In general, slower molecular tumbling (larger τ_R) results in increased relaxivity. In this way, the stimuli-responsive self-assembly of CAs, or the binding of CAs to macromolecules, act as molecular switching processes.[4,8–10]

Intelligent polymers have been developed for various biomedical applications, including drug delivery carriers,[11,12] imaging tools,[13,14] bio-mimic antibodies,[15] and antibacterial agents.[16] Their intelligent behaviors are also applicable to the development of switchable CAs and can be divided broadly into two types of behaviors, resulting from either linear or spherical polymers.

Previously, we applied the morphological change of a linear polymer to the development of a pH-responsive CA.[10] Although spherical polymers also have significant potential to develop switchable CAs, their applicability in this arena has not yet been examined. Herein, we demonstrate that pH-responsive morphological changes of spherical polymers can act as a molecular switching process. Three types of CAs were synthesized using one linear and two different spherical polymers. The relaxivities of these CAs were in fact dependent upon pH. The fluorescence studies indicated that the molecular switch is based on the alteration of the molecular tumbling caused by the pH-responsive morphological changes.

* Corresponding author. Tel.: +81 6 6879 7924; fax: +81 6 6879 7875.
E-mail address: kkikuchi@mls.eng.osaka-u.ac.jp (K. Kikuchi).

0968-0896/$ - see front matter © 2011 Elsevier Ltd. All rights reserved.
doi:10.1016/j.bmc.2011.12.005

2. Results and discussion

2.1. Development of pH-responsive CAs

2.1.1. Design, synthesis, and characterization

To establish a new approach for the development of switchable CAs, we designed three types of pH-responsive CAs, namely **H-Gd**, **C10-Gd**, and **C30-Gd** (Fig. 1). These CAs are based on anionic pH-responsive polymers with Gd^{3+} complexes and dansyl fluorophores. Because it is based on a non-cross-linked homopolymer, the structure of **H-Gd** is considered to be linear. In contrast, **C10-Gd** and **C30-Gd** are spherical structures based on 10% and 30% cross-linked copolymers, respectively. We expected that pH-responsive morphological changes of the polymers could act as molecular switches for the detection of pH change.

According to Scheme 1, we synthesized three types of pH-responsive CAs. Methacrylic acid (MAA) and *N*,*N*′-methylenebisacrylamide (MBAAm) were used as the monomer and cross-linker, respectively. First, non-cross-linked homopolymer PMAA and cross-linked copolymers C10 and C30 were synthesized by distillation precipitation polymerization.[17] The cross-linking degree was controlled by altering the weight of added MBAAm as the appropriate fraction of the combined weight of the monomer and cross-linker. **H-Gd**, **C10-Gd**, and **C30-Gd** were then synthesized by covalently-attaching both the aminoethyl-modified Gd(DO3A) complex [Gd(AEDO3A)],[18] which is a derivative of clinically-used $Gd(DOTA)^{-1}$ complexes, and dansyl ethylenediamine[19] to PMAA, C10, and C30, respectively (Table 1).

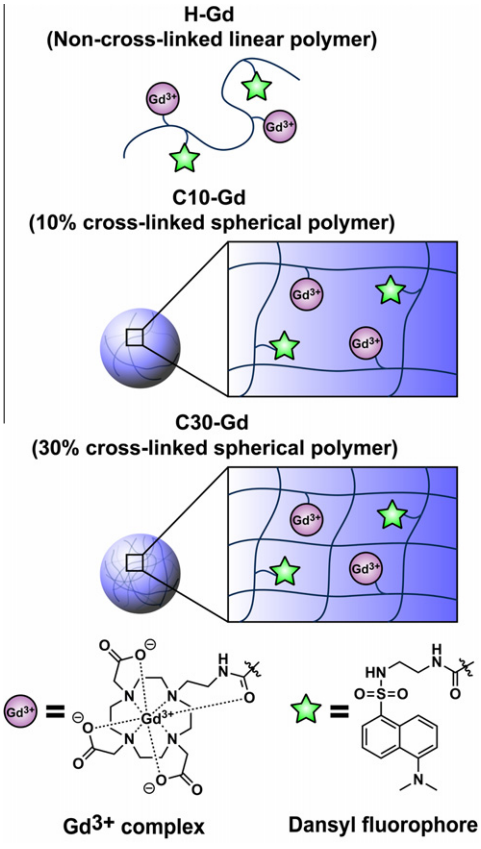

Figure 1. Design of pH-responsive CAs based on the linear homopolymer and cross-linked spherical polymers.

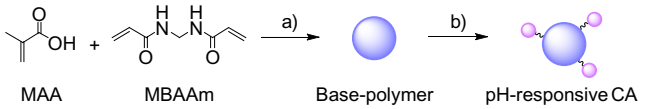

Scheme 1. Synthesis of pH-responsive CAs: (a) AIBN, CH_3CN. (b) Gd(AEDO3A), dansyl ethylenediamine, WSCD·HCl, HOBt, DIEA, DMF.

Table 1
Cross-linking degree, number-average diameter (D_n), weight-average diameter (D_W), polydispersity index (PDI), and Gd content of polymers

Entry	Cross-linking degree[a] (wt %)	D_n[b] (nm)	D_W[b] (nm)	PDI[b]	Gd content (wt %)
PMAA	0	108	114	1.055	0
H-Gd	0	—	—	—	0.21
C10-Gd	10	171	175	1.019	0.42
C30-Gd	30	105	106	1.012	0.45

[a] Calculated from elemental analysis data.
[b] Calculated from TEM images based on the following equation:[17]

$$D_n = \sum_{i=1}^{k} n_i D_i / \sum_{i=1}^{k} n_i ; D_w \sum_{i=1}^{k} n_i D_i^4 / \sum_{i=1}^{k} n_i D_i^3 ; \mathrm{PDI} = D_w / D_n$$

These values reflect the 100 particles from TEM micrographs.

The dispersities, geometries, and average diameters of the synthesized CAs were characterized by transmission electron microscopy (TEM) (Fig. 2 and Table 1). The TEM images showed monodisperse spherical shapes of **C10-Gd** and **C30-Gd**. **H-Gd** was not observed by TEM since it was not cross-linked and was thus expected to become uncoiled during the synthesis and purification process; however, the TEM image of its precursor PMAA was observed. The pH-responses of **C10-Gd** and **C30-Gd** were analyzed under various pH conditions with dynamic light scattering (DLS) (Fig. 3), which showed that the hydrodynamic diameters of **C10-Gd** and **C30-Gd** decreased with decreasing pH. The pH-response of **C10-Gd** was larger than that of **C30-Gd** due to the lower degree of cross-linking of **C10-Gd**. The amount of Gd in each of the polymers was quantified by inductively coupled plasma mass spectrometry (ICP-MS).

2.1.2. Relaxivity measurements

In order to study the function of **H-Gd**, **C10-Gd**, and **C30-Gd** as switchable CAs, we measured their relaxivities using a 0.47 T nuclear magnetic resonance (NMR) analyzer under various pH conditions (Fig. 4). Both r_1 and r_2 of all three polymers increased with decreasing pH, meaning that they all act as pH-responsive CAs and could detect a low pH. The spherical **C10-Gd** and **C30-Gd** showed more drastically varying relaxivity pH-responses than did **H-Gd**. It was also observed that the relaxivity was enhanced by an increase in the degree of cross-linking.

Previously, we developed a pH-responsive CA based on another linear polymer with carboxylate anionic groups.[10] In the study, it was indicated that the pH-responsive morphological conversion between the globular form and the extended form altered the molecular motion of the polymer side chains, and functioned as the molecular switch. The relaxivities of **H-Gd** showed quite similar pH-responsive behaviors to those of the previous polymer. Therefore, pH-responsive relaxometric behaviors of **H-Gd** were probably caused by the molecular motion switch.

The relaxivities of cross-linked spherical **C10-Gd** and **C30-Gd** also increased at low pH. The relaxivity values of the spherical polymers were much higher than those of the linear polymer and enhanced with increasing the cross-linking degree. These results indicate that spherical polymers have significant potential to be switchable CAs with high sensitivities. From DLS measurements, spherical polymers expressed pH-responsive shrinking-swelling behaviors (Fig. 3).

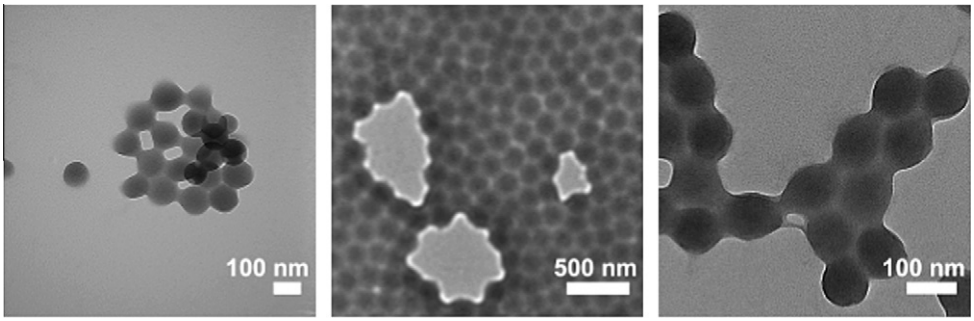

Figure 2. TEM images of PMAA (left), **C10-Gd** (middle), and **C30-Gd** (right).

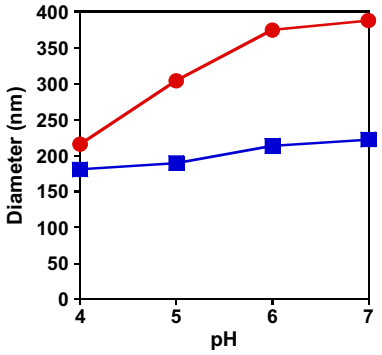

Figure 3. Hydrodynamic diameters of **C10-Gd** (circle symbol) and **C30-Gd** (square symbol) under various pH conditions at 25 °C.

It was assumed that these morphological changes affected the relaxivity. Therefore, the correlations among relaxivities, morphological behaviors, and rotational motions were thoroughly investigated in the following sections (Sections 2.2 and 2.3).

2.2. Elucidation of pH-responsive morphological changes by fluorescence studies

2.2.1. Fluorescence spectra measurements

The dansyl group is an environmentally-sensitive fluorophore that is suitable for observing the pH-response of polymers, because its emission wavelength is blue-shifted as the surrounding hydrophobicity increases, but is negligibly affected by the solution pH.[10,20,21] In order to monitor the pH-responsive morphological change, we measured the fluorescence spectra (Fig. 5). In all polymers, the emission spectra were blue-shifted at a low pH, indicating that the dansyl groups were surrounded by more hydrophobic environment at a low pH. It was expected that **H-Gd** would be a globular structure at a low pH. From the DLS measurements, spherical **C10-Gd** and **C30-Gd** were shown to gradually shrink with a decreasing pH. Thus, it was expected that the increased hydrophobicity of the internal space at a low pH was a result of decreasing the polymer mesh size. The pH-response of **C30-Gd** was smaller compared with the others because its structure is more rigid, owing to its high degree of cross-linking. Interestingly, the wavelength shift of **C10-Gd** was more similar to that of **H-Gd**, rather than **C30-Gd**.

2.2.2. Fluorescence lifetime measurements

The fluorescence lifetime of dansyl fluorophores in the hydrophobic and hydrophilic environments respectively expresses long and short lifetimes.[22] Therefore, the fluorescence lifetime analysis provides the morphological information about the polymer with dansyl groups. We measured the fluorescence decay curves of each of the three CAs at various pH conditions (Supplementary Fig. S1). The fluorescence decay curve of **H-Gd** consisted of two components (Table 2). The first is short lifetime, (~6.7 ns) and its fraction decreased with decreasing pH. The other component is long lifetime (~21.7 ns), which increased with decreasing pH. These results confirm that a higher number of dansyl groups are exposed to the hydrophobic environment as the pH decreases, since **H-Gd** is globular at a lower pH.

In the case of **C10-Gd** and **C30-Gd**, we eliminated the light-scattering lifetime from the calculations for the fractions of each fluorescence lifetime (Table 2). We found that the fluorescence decay parameters of **C10-Gd** were similar to those of **H-Gd**. Although **C10-Gd** is a cross-linked spherical polymer, the surrounding environment of dansyl groups is similar to that of dansyl groups

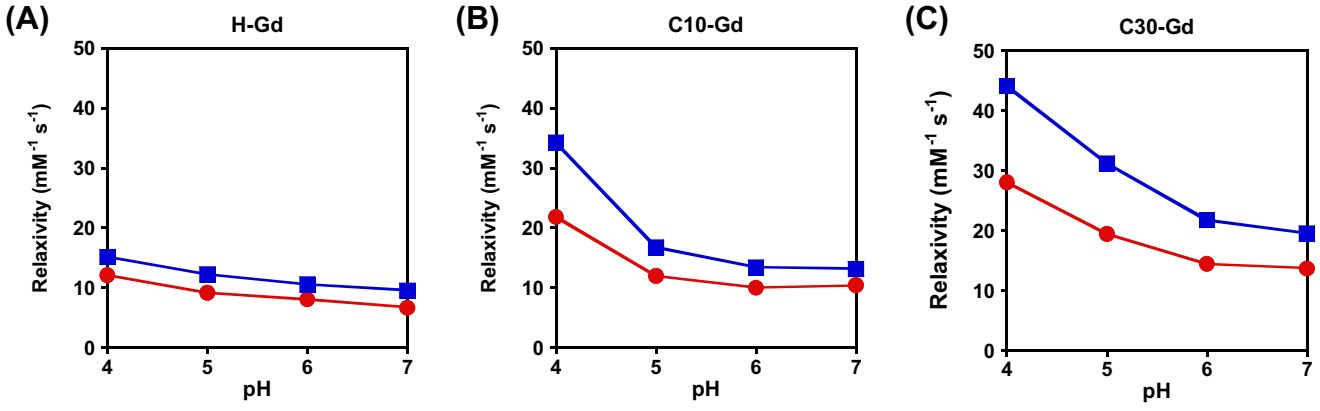

Figure 4. Longitudinal relaxivities (r_1) and transverse relaxivities (r_2) of **H-Gd** (A), **C10-Gd** (B), and **C30-Gd** (C) under various pH conditions at 25 °C. The circle and square symbols represent r_1 and r_2, respectively. The concentration of Gd is presented in mM.

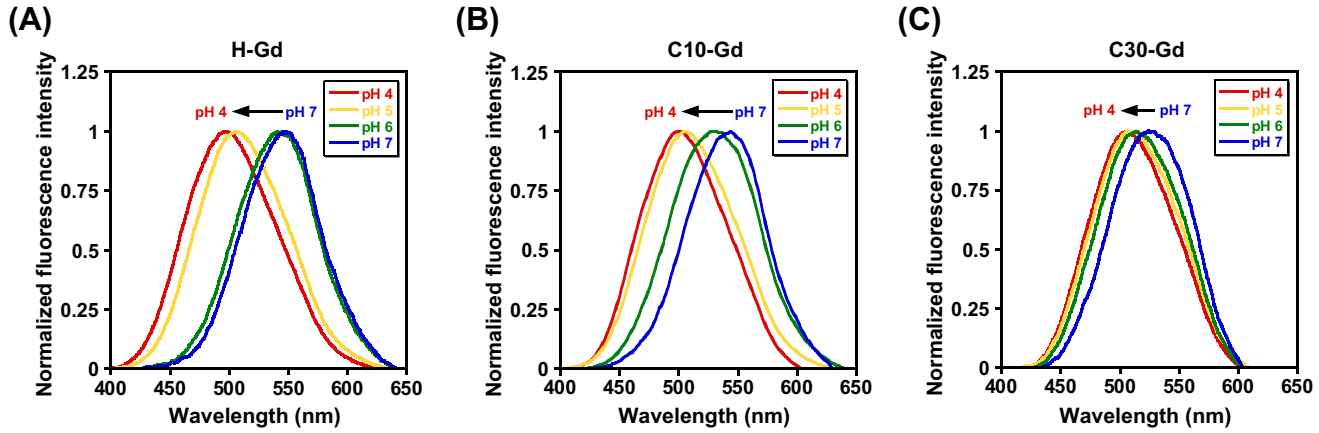

Figure 5. Fluorescence spectra of **H-Gd** (A), **C10-Gd** (B), and **C30-Gd** (C) at 25 °C. λ_{ex} = 330 nm. Red, yellow, green, and blue lines represent pH 4, 5, 6, and 7, respectively.

Table 2
Fluorescence decay parameters of **H-Gd**, **C10-Gd**, and **C30-Gd** under various pH conditions

pH	H-Gd		C10-Gd		C30-Gd	
	τ_1, τ_2 (ns)	F_1, F_2[a] (%)	τ_1, τ_2 (ns)	F_1, F_2[a] (%)	τ_1, τ_2 (ns)	F_1, F_2[a] (%)
4	5.7, 21.7	16, 84	7.1, 20.4	19, 81	7.8, 19.9	22, 78
5	6.7, 21.4	19, 81	7.2, 20.8	23, 77	7.2, 20.0	23, 77
6	3.4, 11.2	86, 14	4.7, 17.0	67, 33	6.3, 19.0	34, 66
7	2.7, 6.3	85, 15	3.5, 11.4	89, 11	5.4, 16.5	56, 44

[a] Fraction (F_i) of τ_i was defined as $100 \times I_i/(I_1 + I_2)$, ($i$ = 1, 2); I_i is the pre-exponential factor (please see Section 4).

attached to a linear polymer. However, the fluorescence decay parameters of **C30-Gd** were found to be quite different from those of **H-Gd** and **C10-Gd**. In **C30-Gd**, the long-lifetime component (τ_2) was almost constant at a pH between 4 and 7, and the pH-responsive change in the fraction of τ_2 was much smaller than that of **H-Gd** and **C10-Gd**. This is most likely due to the rigid structure of **C30-Gd,** which results from the high degree of cross-linking, making the surrounding environment of dansyl groups less susceptible to changes in pH. These results were consistent with the results from DLS and fluorescence spectra.

Fluorescence lifetimes (τ_F) were calculated as weighted average values based on τ_1 and τ_2 (please see the Section 4). Calculated τ_F was shown to increase with decreasing pH (Fig. 6), and the τ_F of **H-Gd** and **C10-Gd** significantly changed between pH 5 and 6.

2.3. Elucidation of the molecular switch mechanism

2.3.1. Fluorescence anisotropy measurements

The fluorescence anisotropy provides information about the molecular motion, in that it increases as the molecular motion of the fluorophores becomes slower. Thus, we measured the fluorescence anisotropies of **H-Gd**, **C10-Gd**, and **C30-Gd** at the wavelength of their emission maximum at each pH (Fig. 7), which showed that the molecular motion of all polymers became slower with a decreasing pH. Moreover, as the cross-linking degree increased, the molecular motion was restricted. These results agreed with our initial hypothesis that the pH-response of the relaxivity is because of the alteration of the molecular motion.

2.3.2. Calculation of rotational correlation time

It is known that rotational correlation time (τ_R) is one of the factors that affect the relaxivity of the CA, and provides quantitative information about the molecular tumbling.[1,23] Therefore, estimating behaviors of τ_R could be significantly helpful in designing and

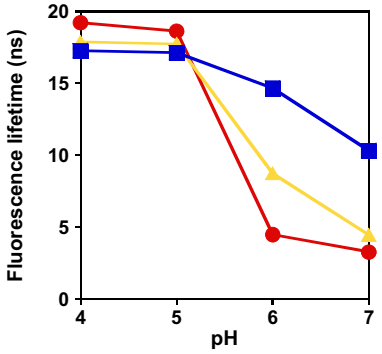

Figure 6. Fluorescence lifetimes of **H-Gd** (circle symbol), **C10-Gd** (triangle symbol), and **C30-Gd** (square symbol) at 25 °C. λ_{ex} = 370 nm. λ_{em} is in the range of 498–548 nm.

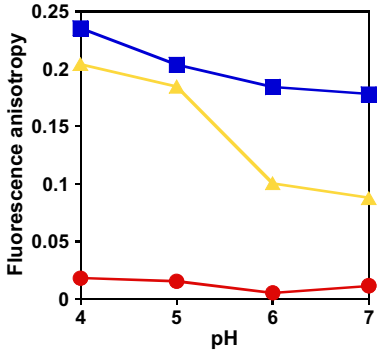

Figure 7. Fluorescence anisotropies of **H-Gd** (circle symbol), **C10-Gd** (triangle symbol), and **C30-Gd** (square symbol) at 25 °C. λ_{ex} = 330 nm. λ_{em} is in the range of 498–548 nm.

developing switchable CAs. The τ_R can be calculated from Perrin-Weber Eq. 1.[21,24]

$$A_0/A = 1 + \tau_F/\tau_R \quad (1)$$

In Eq. 1, A and τ_F represent the fluorescence anisotropy and fluorescence lifetime, respectively. A_0 is the limiting fluorescence anisotropy when no rotational diffusion occurs. The A_0 of dansyl fluorophores was experimentally determined to be 0.325 by Hu et al.[25]

The τ_R was calculated using measured values of A and τ_F (Fig. 8 and Supplementary Table S1–3), and the pH-response of τ_R was

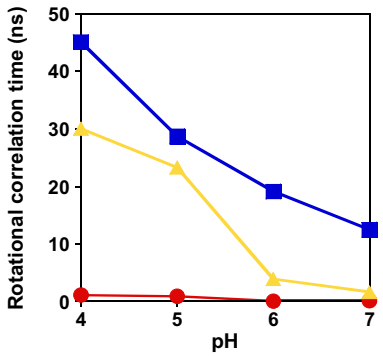

Figure 8. Rotational correlation times of **H-Gd** (circle symbol), **C10-Gd** (triangle symbol), and **C30-Gd** (square symbol) at 25 °C.

shown to be highly correlated with that of relaxivity. This result indicates that pH-responsive τ_R alterations caused changes in the relaxivities. Moreover, τ_R values of cross-linked **C10-Gd** and **C30-Gd** were much higher than those of **H-Gd**. Thus, it was expected that the relaxivity enhancement of cross-linked polymers was result of the increase of τ_R values. The linear structure is assumed to be a two-dimensional structure. As a result, the side chains can move relatively freely from the polymer backbone. In contrast, the cross-linked spherical shape is a three-dimensional structure, the inside of which is like highly wired polymer network. This network restricts the free movement of the side chains and extends the τ_R values.

Although **C30-Gd** expressed the small morphological change at low pH (Fig. 3 and Fig. 5), the relaxivities drastically increased at the pH region. Since the τ_R values of **C30-Gd** significantly increased at low pH (Fig. 8), it is expected that 30% of the cross-linking little restricts the pH-response in the local molecular tumbling, but it highly restricts that in the entire morphology.

The τ_R of **H-Gd** were below 1.1 ns and significant smaller than previous results obtained from a linear polymer with hydrophobic octyl groups, the maximum τ_R value of which is 12.8 ns at pH 4.[10] Nevertheless, the relaxivity values of **H-Gd** were maintained close to those of previous one. It is likely that the absence of hydrophobic groups and the difference of buffer conditions caused high relaxivities of **H-Gd** despite its fast molecular tumbling.

In summary, fluorescence studies and following calculation of τ_R values indicated that pH-responsive morphological changes in **H-Gd**, **C10-Gd**, and **C30-Gd** altered the rotational motion of their side chains, and caused their relaxivity switch properties. These results also demonstrated that spherical cross-linked polymers have more significant applicability to the design of switchable CAs, because increase of the cross-linking degree induced the relaxivity enhancement by restricting the molecular tumbling while maintaining the switching property (Fig. 9).

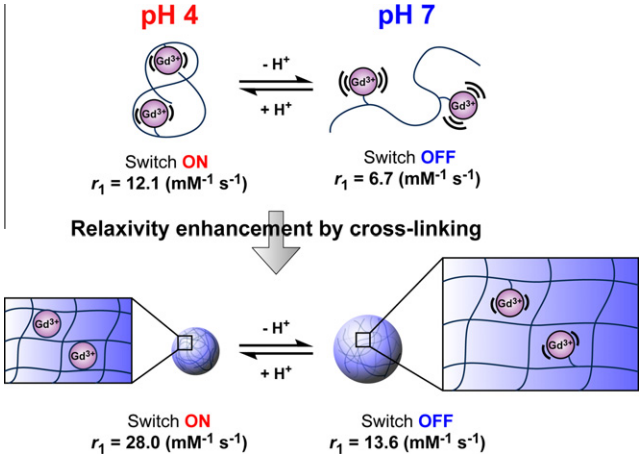

Figure 9. Proposed principle of molecular switches of **H-Gd** and **C30-Gd**.

3. Conclusions

Here, we applied morphological changes of pH-responsive polymers as a novel molecular switching process for MRI. The pH-responsive CAs were developed by attaching Gd^{3+} complexes and dansyl fluorophores to a linear homopolymer or spherical polymers. The relaxivities of the all polymers increased with a decreasing pH. The fluorescence studies indicated that the relaxivity change of the polymers is due to the alteration of the molecular correlation time τ_R caused by the pH-responsive morphological changes. A higher degree of cross-linking enhanced the relaxivities while maintaining the switching response; therefore, the cross-linked spherical polymers were found to be promising materials for the development of switchable CAs. Since such intelligent behaviors of spherical polymers have recently attracted much attention in the field of drug delivery,[11,26] our novel approaches also could lead to valuable biomedical applications in combination with drug delivery systems.

4. Experimental section

4.1. General procedures

The chemicals used in these experiments were obtained from Tokyo Chemical Industries, Wako Pure Chemical, and Aldrich Chemical Company. Because all the materials were purchased at the highest grade available, they were used without further purification. NMR spectra were recorded on a JEOL JNM-AL400 instrument at 400 MHz for ^1H and at 100.4 MHz for ^{13}C with tetramethylsilane as an internal standard. ESI-TOF MS were taken on a Waters LCT-Premier XE. Relaxation times were measured on a Bruker Optics minispec mq20. The inversion-recovery sequence and Carr–Purcell–Meiboom–Gill sequence were used for the measurements of T_1 and T_2, respectively. The r_1 and r_2 were respectively determined from the slopes obtained by plotting at least four points of $1/T_1$ and $1/T_2$ versus the concentration of the CA. Fluorescence spectra and fluorescence anisotropy were measured using a Hitachi F4500 spectrometer. Fluorescence decays were measured using a Horiba TemPro. DLS was performed using a Horiba SZ-100. TEM was performed using a Hitachi H-800 operated at 200 kV. ICP-MS were taken on an Agilent Technologies 7500cs.

Twice-diluted McIlvaine buffers (pH 4–7) were used as solutions for the pH adjustment and were prepared by mixing an arbitrary amount of 0.1 M citric acid aqueous solution with a 0.2 M disodium hydrogen phosphate aqueous solution.

4.2. Synthesis

4.2.1. PMAA, C10, and C30

Polymers were synthesized by distillation precipitation polymerization with a slight alteration, as follows.[17] For the synthesis of C10, 598 mg (6.95 mmol) of MAA, 32 mg (0.21 mmol) of MBAAm cross-linker (5 wt % of total monomer and cross-linker), and 13 mg (0.079 mmol) of 2,2′-azobisisobutyronitrile (AIBN) initiator (2 wt % of total monomer and cross-linker) were dissolved in 80 mL of acetonitrile in a dried two-neck flask fitted with a fractionating column, a condenser, and a receiving flask. The mixture was kept under an argon atmosphere and heated from room temperature

to boiling state within 15 min. Polymerization was performed until approximately 40 mL of acetonitrile was distilled from the reaction system within 60 min. The product was then purified three times by the following processes: centrifugation, decantation, and resuspension in acetonitrile with ultrasonication. The purified product was dissolved in distilled water and filtered through a Millipore 0.8 μm filter. The filtrate was freeze-dried, and a white powder was obtained. C30 was synthesized by altering the amount of MBAAm to 20 wt % of the combined weight of monomer and cross-linker. In the case of PMAA, no cross-linker was added to the reaction mixture. The amounts of total monomer and cross-linker were maintained at 1 wt % relative to the reaction medium, and the amounts of AIBN were maintained at 2 wt % relative to the total monomer and cross-linker.

4.2.2. H-Gd, C10-Gd, and C30-Gd

For the synthesis of **H-Gd**, 100 mg of PMAA was dissolved in 20 mL of anhydrous *N*,*N*-dimethylformamide (DMF) in a three-neck flask and stirred under argon. 267 mg (1.39 mmol) of 1-ethyl-3-(3-dimethylaminopropyl)carbodiimide hydrochloride (WSCD·HCl), 188 mg (1.39 mmol) of 1-hydroxybenzotriazole (HOBt), and 180 mg (1.39 mmol) of *N*,*N*-diisopropylethylamine (DIEA) were added to the solution. The molar quantity of these reagents was maintained at 1.2 equiv of carboxyl groups of the polymer. After 30 min, 3.0 mg (0.0050 mmol, 2.5 wt % of the weight of the polymer) of Gd(AEDO3A) and 2.0 mg (0.0070 mmol, 2.0 wt % of the weight of the polymer) of dansyl ethylenediamine were added to the mixture, which was stirred overnight at room temperature. The DMF was then evaporated under reduced pressure, and a yellow oil was obtained. The residue was dissolved in 1.0 M NaOH aq and then neutralized by 1.0 M HCl aq. The solution was purified by ultrafiltration using a Sartorius VIVASPIN (MWCO 3000). The supernatant was freeze-dried, and a white powder was obtained.

The synthetic procedures for **C10-Gd** and **C30-Gd** were identical to that of **H-Gd,** but required a different purification process. After the evaporation of DMF, **C10-Gd** and **C30-Gd** were purified by performing the following processes five times: centrifugation, decantation, and resuspension in methanol with ultrasonication. The products were then dissolved in 1.0 M NaOH aq and neutralized by 1.0 M HCl aq. Next, the solutions were centrifuged and washed with distilled water several times. The purified products were freeze-dried, and white powders were obtained.

Gd(AEDO3A) and dansyl ethylenediamine were synthesized according to previous reports.[18,19]

4.3. Fluorescence lifetime measurements

The fluorescence decay curve of **H-Gd** was acquired and fitted to the double-exponential Eq. 2. In the case of **C10-Gd** and **C30-Gd**, fluorescence decay curves were fitted with triple-exponential components because of the light scattering light.

$$I(t) = I_1 exp(-t/\tau_1) + I_2 exp(-t/\tau_2) \quad (2)$$

The weighted average fluorescence lifetime (τ_F) was calculated using Eq. 3 by excluding the light scattering component. The lifetime of the scattering light was on the tens of picoseconds timescale, which is much shorter than the nanosecond timescale of the fluorescence lifetime.

$$\tau_F = \tau_1 I_1/(I_1 + I_2) + \tau_2 I_2/(I_1 + I_2) \quad (3)$$

Acknowledgments

This work was partially supported by the Japan Society for the Promotion of Science (JSPS) through its 'Funding Program for World-Leading Innovative R&D on Science and Technology (FIRST) Program' and by the Ministry of Education, Culture, Sports, Science, and Technology (MEXT) of Japan (Grant No. 20675004, 21685019, and 22108519). The Takeda Science Foundation, the Mochida Memorial Foundation, and the Naito Foundation also provided support. The Asahi Glass Foundation provided financial support. Part of the present experiments was carried out in a facility at the Research Center for Ultra-High Voltage Electron Microscopy at Osaka University. S.O. received support from the Global COE Program 'Global Education and Research Center for Bio-Environmental Chemistry' of Osaka University and the JSPS Fellowship for Young Scientists.

Supplementary data

Supplementary data associated with this article can be found, in the online version, at doi:10.1016/j.bmc.2011.12.005.

References and notes

1. Lauffer, R. B. *Chem. Rev.* **1987**, *87*, 901.
2. Jun, Y.-w.; Lee, J.-H.; Cheon, J. *Angew. Chem., Int. Ed.* **2008**, *47*, 5122.
3. Louie, A. Y.; Hüber, M. M.; Ahrens, E. T.; Rothbächer, U.; Moats, R.; Jacobs, R. E.; Fraser, S. E.; Meade, T. J. *Nat. Biotechnol.* **2000**, *18*, 321.
4. Hanaoka, K.; Kikuchi, K.; Terai, T.; Komatsu, T.; Nagano, T. *Chem. Eur. J.* **2008**, *14*, 987.
5. Zhang, X.-A.; Lovejoy, K. S.; Jasanoff, A.; Lippard, S. J. *Proc. Natl. Acad. Sci. U.S.A.* **2007**, *104*, 10780.
6. Que, E. L.; Gianolio, E.; Baker, S. L.; Wong, A. P.; Aime, S.; Chang, C. J. *J. Am. Chem. Soc.* **2009**, *131*, 8527.
7. Zhang, S.; Wu, K.; Sherry, A. D. *Angew. Chem., Int. Ed.* **1999**, *38*, 3192.
8. Tóth, É.; Bolskar, R. D.; Borel, A.; González, G.; Helm, L.; Merbach, A. E.; Sitharaman, B.; Wilson, L. J. *J. Am. Chem. Soc.* **2005**, *127*, 799.
9. Aime, S.; Fedeli, F.; Sanino, A.; Terreno, E. *J. Am. Chem. Soc.* **2006**, *128*, 11326.
10. Okada, S.; Mizukami, S.; Kikuchi, K. *ChemBioChem* **2010**, *11*, 785.
11. Hu, Y.; Litwin, T.; Nagaraja, A. R.; Kwong, B.; Katz, J.; Watson, N.; Irvine, D. J. *Nano Lett.* **2007**, *7*, 3056.
12. Yang, X.; Chen, L.; Huang, B.; Bai, F.; Yang, X. *Polymer* **2009**, *50*, 3556.
13. Gota, C.; Okabe, K.; Funatsu, T.; Harada, Y.; Uchiyama, S. *J. Am. Chem. Soc.* **2009**, *131*, 2766.
14. Tanaka, K.; Kitamura, N.; Chujo, Y. *Macromolecules* **2010**, *43*, 6180.
15. Hoshino, Y.; Koide, H.; Urakami, T.; Kanazawa, H.; Kodama, T.; Oku, N.; Shea, K. J. *J. Am. Chem. Soc.* **2010**, *132*, 6644.
16. Oda, Y.; Kanaoka, S.; Sato, T.; Aoshima, S.; Kuroda, K. *Biomacromolecules* **2011**, *12*, 3581.
17. Liu, G.; Yang, X.; Wang, Y. *Polym. Int.* **2007**, *56*, 905.
18. Li, C.; Li, Y.-X.; Law, G.-L.; Man, K.; Wong, W.-T.; Lei, H. *Bioconjugate Chem.* **2006**, *17*, 571.
19. Shea, K. J.; Stoddard, G. J.; Shavelle, D. M.; Wakui, F.; Choate, R. M. *Macromolecules* **1990**, *23*, 4497.
20. Hu, Y.; Smith, G. L.; Richardson, M. F.; McCormick, C. L. *Macromolecules* **1997**, *30*, 3526.
21. Hu, Y.; Armentrout, R. S.; McCormick, C. L. *Macromolecules* **1997**, *30*, 3538.
22. Li, Y.-H.; Chan, L.-M.; Tyer, L.; Moody, R. T.; Himel, C. M.; Hercules, D. M. *J. Am. Chem. Soc.* **1975**, *97*, 3118.
23. Caravan, P. *Chem. Soc. Rev.* **2006**, *35*, 512.
24. Weber, G. *Biochem. J.* **1952**, *51*, 145.
25. Hu, Y.; Horie, K.; Ushiki, H. *Macromolecules* **1992**, *25*, 6040.
26. Oishi, M.; Hayashi, H.; Iijima, M.; Nagasaki, Y. *J. Mater. Chem.* **2007**, *17*, 3720.